JACS
JOURNAL OF THE AMERICAN CHEMICAL SOCIETY
Article
pubs.acs.org/JACS

High-Strength, Healable, Supramolecular Polymer Nanocomposites

Justin Fox,[†] Jeong J. Wie,[‡] Barnaby W. Greenland,[§] Stefano Burattini,[§] Wayne Hayes,[§] Howard M. Colquhoun,[§] Michael E. Mackay,*[,‡,∥] and Stuart J. Rowan*[,†]

[†]Department of Macromolecular Science and Engineering, Case Western Reserve University, 2100 Adelbert Road, Kent Hale Smith Building, Cleveland, Ohio 44106, United States

[‡]Department of Chemical Engineering, University of Delaware, 150 Academy Street, Newark, Delaware 19716, United States

[§]Department of Chemistry, University of Reading, Whiteknights, Reading, RG6 6AD, U.K.

[∥]Department of Materials Science & Engineering, University of Delaware, 201 DuPont Hall, Newark, Delaware 19716, United States

Supporting Information

ABSTRACT: A supramolecular polymer blend, formed via $\pi-\pi$ interactions between a π-electron rich pyrenyl end-capped oligomer and a chain-folding oligomer containing pairs of π-electron poor naphthalene-diimide (NDI) units, has been reinforced with cellulose nanocrystals (CNCs) to afford a healable nanocomposite material. Nanocomposites with varying weight percentage of CNCs (from 1.25 to 20.0 wt %) within the healable supramolecular polymeric matrix have been prepared via solvent casting followed by compression molding, and their mechanical properties and healing behavior have been evaluated. It is found that homogeneously dispersed films can be formed with CNCs at less than 10 wt %. Above 10 wt % CNC heterogeneous nanocomposites were obtained. All the nanocomposites formed could be rehealed upon exposure to elevated temperatures although, for the homogeneous films, it was found that the healing rate was reduced with increasing CNC content. The best combination of healing efficiency and mechanical properties was obtained with the 7.5 wt % CNC nanocomposite which exhibited a tensile modulus enhanced by as much as a factor of 20 over the matrix material alone and could be fully rehealed at 85 °C within 30 min. Thus it is demonstrated that supramolecular nanocomposites can afford greatly enhanced mechanical properties relative to the unreinforced polymer, while still allowing efficient thermal healing.

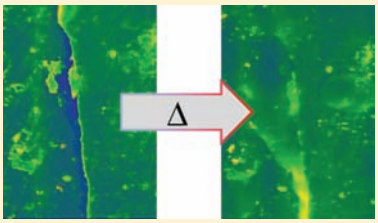

INTRODUCTION

Polymers with the capability to undergo healing have enjoyed significant attention in recent years,[1−6] due to the potential advantages they offer including greatly extended application lifetimes and reduced maintenance.[7] A variety of approaches have emerged over the past decade to access healable materials, and they can be broadly classified as either autonomous self-healing systems, which include methods using encapsulated monomers that are released and polymerized upon material damage,[8,9] or stimuli-responsive rehealable systems, such as thermally reversible covalent bond-forming moieties engineered into the polymer backbone.[10] Of primary interest here are materials that utilize reversible, noncovalent interactions to elicit a healing response. Generally, in such supramolecular systems low molecular weight molecules self-assemble into polymeric aggregates through specific noncovalent bonds. Two properties of supramolecular polymers (and also of dynamic covalent systems)[11−16] that lend themselves to rapid and controllable healing are the stimuli responsiveness of the reversible (dynamic) bond[17] and the high diffusion constants of oligomeric species.[18] Given the variety of reversible interactions that can be used in the design of a supramolecular healable material, many elegant and creative solutions have been explored including materials that respond to external stimuli such as heat,[19,20] pressure,[19,21,22] water,[23] or light.[24]

However, a leading drawback with the current generation of healable supramolecular materials is their generally low mechanical strength. In previous studies, we have explored dynamic motifs that utilize supramolecular $\pi-\pi$-stacking interactions in a number of different rehealable materials.[25−27]

In particular, we have utilized the interaction between an oligomer terminated at both ends by π-electron rich pyrenyl moieties and a second, chain-folding oligomer having a series of "tweezer" moieties based on pairs of π-electron poor naphthalene-diimide (NDI) units separated by a simple triethyleneoxy residue.[28] In these studies, we have shown that, at equimolar ratios of the two binding motifs, blends of polydiimide (**1**) and the pyrene end-capped polyamide (**2**) form stable, compatible, freestanding films with the ability to undergo rapid and complete healing when annealed above 50 °C.[25b] Initial tensile testing of **1**·**2** revealed an extensible material with failure typically occurring at around 75% strain. However, this ductility is accompanied by a relatively low tensile modulus (<10 MPa).

In subsequent studies we have found that increasing the strength of the supramolecular binding motif (primarily by increasing the number of $\pi-\pi$ interactions) results in enhanced mechanical properties.[26] However, in such systems, improved

Received: January 3, 2012
Published: March 9, 2012

   dx.doi.org/10.1021/ja300050x | J. Am. Chem. Soc. 2012, 134, 5362−5368

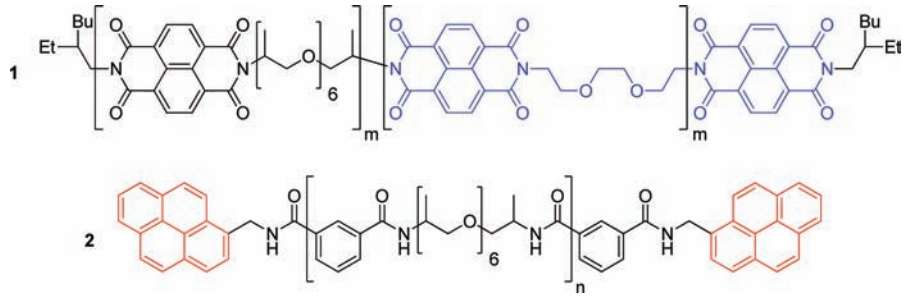

Figure 1. Molecular structure of healing polymer blend **1·2** (1:3 w/w ratio).[23]

mechanical behavior comes at the expense of increased time and temperature required to achieve 100% recovery in tensile strength on healing. An alternative approach that is commonly used to enhance the mechanical properties of a polymer is to use a reinforcing (nano)filler.[29−31] However, to date, data reporting the use of nanofillers to mechanically reinforce a healable supramolecular polymer have not been described in the literature. In the present study we have investigated nanocomposites of a healable, supramolecular polymer matrix and examined the effect that the nanofiller has on both the mechanical strength and the healing properties of this system.

Nanocomposites utilizing cellulose nanocrystals (CNCs or cellulose whiskers) are another burgeoning area of research.[32] CNCs are attractive as reinforcing fillers because of their high tensile stiffness (up to ca. 140 GPa), relative abundance in nature, and low density.[33] They can be obtained from a range of biosources (e.g., cotton, wood, wheat straw, or sea creatures known as tunicates) and can vary in aspect ratio (*ca.* 10 to 100) depending on the biosource.[34] A wide range of polymer matrices have been shown to be reinforced by CNCs from soft matrices such as poly(ethylene oxide-*co*-epichlorohydrin)[35] and low density polyethylene[36] to hard epoxy resins.[37] All these systems exhibited greatly improved stiffness values over the corresponding matrix materials, which has been related, in part, to the strong interactions (i.e., hydrogen bonding) exhibited between the fibers. Herein we detail the production, mechanical properties, and healing behavior of a series of nanocomposites comprised of the healable polymer blend **1·2** (1:3 w/w ratio) reinforced with varying weight percentages of CNC nanofiller (Figure 1). It is expected that there will also be significant matrix−fiber interactions given the presence of a number of hydrogen bond accepting moieties in the matrix polymer blend.

EXPERIMENTAL SECTION

Materials. All solvents and reagents were purchased from Aldrich Chemical Co. and used without further purification. The healable polymer blend **1·2** (1:3 w/w ratio) was prepared according to literature procedures.[25]

Instruments and Procedures. CNCs were isolated from the cellulose mantles of sea tunicates after hydrolysis with sulfuric acid, using established techniques.[38,39] Two stock suspensions of CNCs (2.0 mg/mL) and **1·2** (1:3 weight ratio, 50 mg/mL) were prepared by adding *N*,*N*-dimethylformamide (DMF) to the solid and then sonicating until stable suspensions were achieved (*ca.* 2 h). Nanocomposite samples were produced by mixing appropriate ratios of the two stock suspensions and then sonicating for a further *ca.* 30 min before casting into PTFE dishes. The DMF was fully removed by placing samples in a vacuum oven under reduced pressure (75 Torr) at room temperature for 24 h. The pressure was further reduced to 20 Torr, and the cosuspensions were then heated to 40 °C for 120 h. Thermogravimetric analysis (TGA) of the resulting films confirmed that all of the DMF had been removed. After casting, films were compression molded between two PTFE sheets in a Carver Model C laboratory press at 85 °C under 200 kPa of pressure, with PTFE spacers of 150 μm around all samples to ensure uniform thickness.

Uniaxial tensile deformation and healing studies were performed at room temperature on a Zwick-Roell Z0.5 TM Materials Testing Machine with a 500 kN load cell and polyurethane sample grips (*ca.* sample geometry [length × width × thickness]: 30.0 × 3.3 × 0.150 mm). Samples were submitted to stress-controlled testing at 100 mN/s with 0.05 N of preload force. Tensile moduli were calculated from the slopes of the linear region between 0.5 and 1.0% strain.

Reprocessing/Healing Procedures. Nanocomposite films were evaluated for their healing ability via two different reprocessing/healing procedures monitored by tensile testing experiments and a third rheological evaluation.

In the first set of experiments the films were cleanly broken during initial tensile testing and were mended by overlapping the broken edges by *ca.* 5 mm and compression molding at 200 kPa between PTFE sheets at 85 °C for 5 min with 150 μm PTFE spacers around the samples. Since these conditions also represent the original processing conditions (i.e., relatively long time and high pressure), samples mended in this way are referred to as "reprocessed". The reprocessed films (3 trials per formulation) were then subjected to the same tensile testing conditions described previously.

A second set of experiments was conducted on a series of freshly processed nanocomposites that were designed to see if the materials could be thermally healed. The process here is a slight variation of the procedure used previously to examine the healing ability of the neat film **1·2**.[25b] Except for controls, samples were bisected with a razor blade crosswise and arranged with a 5 mm overlap on a PTFE sheet. Samples (including intact control samples) were then heated for 2, 5, 10, or 20 min in an oven at 85 °C. After removal from the oven, each sample was quickly cooled on a water-chilled aluminum heat sink and subjected to tensile testing. Three samples of each nanocomposite at each time period (12 rehealed samples total plus three controls) were prepared and tested.

For the rheological study, nanocomposite films were punch-pressed into 8 mm disks. All rheological measurements were conducted with a strain control rheometer ARES-G2 (TA Instruments) using 8 mm parallel plates. In order to ensure good contact between samples and plates, all samples were heated to 100 °C at either 1 N (for **1·2** and the 1.25 wt % nanocomposite), 3 N (for the 2.5, 10, and 20 wt % nanocomposites), or 5 N (for the 7.5 wt % nanocomposite) of force for 5 min prior to testing.

Scanning Electron Microscopy (SEM) Studies. Fractured samples were heated progressively from room temperature to 200 °C in the SEM, at a heating rate of 5 °C min^{-1}, on the variable temperature (VT) stage of an FEI Quanta FEG 600 Environmental Scanning Electron Microscope, with images recorded at 20 °C intervals.

RESULTS AND DISCUSSION

For this study, we chose to utilize CNCs isolated from the sessile sea creatures known as tunicates (*styela clava*). CNCs from this biosource have high stiffness values (tensile modulus of ca. 140 GPa[33]) and one of the highest aspect ratios of the

dx.doi.org/10.1021/ja300050x | *J. Am. Chem. Soc.* 2012, 134, 5362−5368

naturally available CNCs (length (l)/ diameter (d) ≈ 80).[40] At this aspect ratio, nanocomposite percolation theory[41] predicts that a sample-spanning network of CNCs can be achieved at a concentration of less than 1% v/v. The CNCs were obtained using previously published procedures,[38,39] via sulfuric acid hydrolysis of the tunicate mantles, and as a consequence the CNC surface is decorated with negatively charged sulfate groups. Transmission Electron Microcopy (TEM) (see Supporting Information, Figure S1) confirms that these isolated CNCs have dimensions (*ca.* 25 nm × 2.1 μm) similar to those obtained from tunicate mantles previously reported.[35] Conductometric titrations of the CNCs used in this study revealed their average surface charge to be 130 mmol/kg (see Supporting Information, Figure S2).

It is important to produce nanocomposites with a homogeneous dispersion of CNCs within the polymer matrix (**1·2**) in order to achieve the greatest enhancement in mechanical properties across the whole film. The best way to achieve this would be to use a common solvent for both the CNCs and the matrix polymer that is subsequently removed to produce a homogeneous blend.[42] However, **1·2** is only soluble in a limited range of solvents (e.g., trichloroethanol or solvent mixtures containing hexafluoroisopropanol).[25] Unfortunately CNCs do not disperse well in such solvent systems. It has previously been shown that CNCs are easily dispersed in dipolar aprotic solvents such as DMF upon sonication.[35,43] While **1·2** does not dissolve in DMF it does form finely dispersed suspensions suitable for solvent casting of the CNC/**1·2** mixtures (Figure 2). After removal of the DMF (vacuum oven over 6 days; see Supporting Information, Figure S3) the films were compression molded at 85 °C and 200 kPa for *ca.* 5 min to obtain a uniform thickness (*ca.* 150 μm) across the range of samples tested. It was noticeable that heat treatment of the solvent-cast films resulted in a change in their mechanical properties (see Supporting Information, Figure S4). This is not a matter of concern since the films are subjected to thermal treatment during the healing process and is necessary to erase the effects of solvent casting to establish a uniform thermal history for the series of nanocomposites. By application of this procedure, films containing 1.25, 2.50, 5.00, 7.50, 10.0, and 20.0 wt % CNC in **1·2** were prepared. However, it should be noted that while we could obtain free-standing, stiff nanocomposite films containing 20 wt % of CNCs (tensile modulus, E = 460 MPa) via solvent casting, compression molding of these materials using the conditions described above led to macroscopic phase segregation and a dramatic decrease in the mechanical stability of the films (see Supporting Information, Figure S5). Thus the 20 wt % samples were not investigated further in the tensile testing studies.

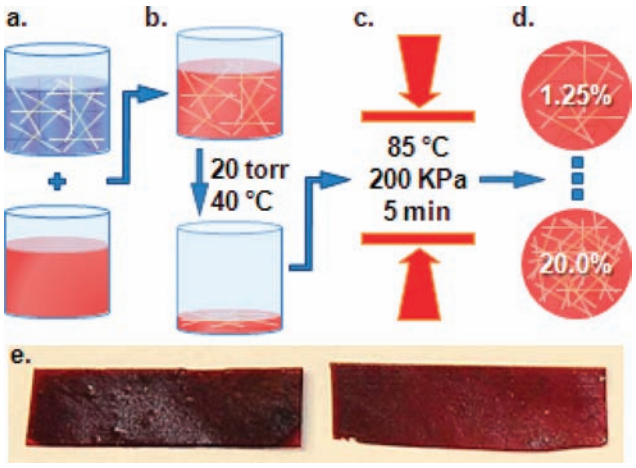

Figure 2. Processing of the nanocomposites begins with (a) mixing and sonication of DMF suspensions of CNC and **1·2** followed by (b) film casting under vacuum and (c) compression molding to yield six nanocomposites (d) containing CNCs at 1.25, 2.5, 5.0, 7.5, 10.0, and 20.0 wt %. Images of 2.50 wt % film (e) after solution casting (left, ca. 250 μm thick) and after compression molding (right, ca. 150 μm thick).

Tensile Data and Reprocessing of the Nanocomposites. A series of stress–strain experiments was carried out to examine the degree of mechanical enhancement imparted by incorporation of the CNC filler into the healable matrix. Figure 3 and Table 1 show the typical stress–strain curves and resulting tensile moduli (E_o, original tensile moduli), respectively, for the matrix polymer and five of the nanocomposites produced via the compression molding process described above. Increasing the percentage of CNC filler within the matrix results in a dramatic increase in the value of E (from *ca.* 8 MPa for the neat matrix to *ca.* 260 MPa for the 10 wt % CNC nanocomposite) along with a significant decrease in extension to break values.

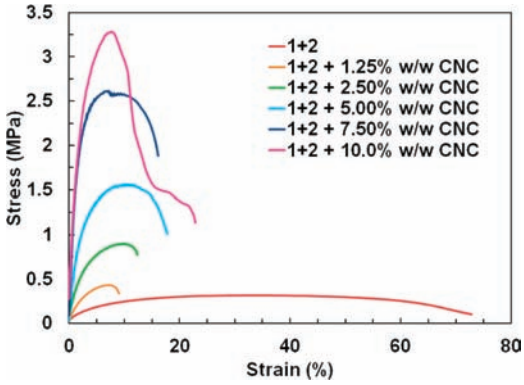

Figure 3. Stress–strain curves across the range of nanocomposites.

Table 1. Tensile Moduli of Original (E_O) and Reprocessed (E_R) Films and Nanocomposites

Sample	E_O (MPa)	E_R (MPa)
1·2	8.0 ± 3.2	8.2 ± 3.6
1·2 + 1.25 wt % CNC	15.4 ± 2.2	13.0 ± 2.1
1·2 + 2.50 wt % CNC	32.7 ± 6.2	29.8 ± 11.9
1·2 + 5.00 wt % CNC	78.6 ± 22.8	64.6 ± 25.2
1·2 + 7.50 wt % CNC	149 ± 33	169 ± 39
1·2 + 10.0 wt % CNC	261 ± 162	341 ± 184

The data are consistent with the mechanical reinforcement in these nanocomposites resulting from the formation of a rigid, percolating network of CNCs within the matrix. To examine this more quantitatively, we compared the data in Table 1 with values based on a Percolation model,[44−46] to see if the degree of mechanical property enhancement matches that predicted for a homogeneously dispersed nanocomposite. By incorporation of the measured tensile modulus of the matrix material (8 MPa), the known modulus (*ca.* 5 GPa[35]) of a sheet of the tunicate CNCs, the aspect ratio of a single CNC of *ca.* 80, and the known volume fraction of CNC in the nanocomposite, the

dx.doi.org/10.1021/ja300050x | J. Am. Chem. Soc. 2012, 134, 5362−5368

mechanical properties of the nanocomposites can be predicted. Figure 4 shows the results of this calculation (blue line) along

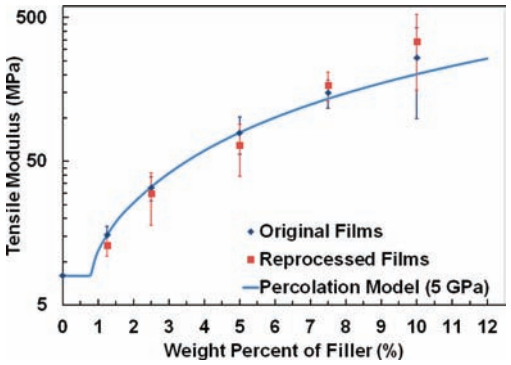

Figure 4. Tensile moduli (E) of undamaged and reprocessed nanocomposite films, along with reinforcement predictions calculated according to the Percolation model.[44]

with tensile moduli of the nanocomposites (blue diamonds). Gratifyingly, the measured E_o values of the nanocomposite match very well (within error) with those predicted by the percolation model. This suggests the nanocomposites have material properties consistent with a uniform dispersion of CNCs within the healable polymer that effectively transfer stress across the films through filler−filler interactions.

It is worth noting, however, that the 10 wt % nanocomposite compared to the other nanocomposites has a tensile modulus with a much larger error. During the compression molding process, the matrix used in these nanocomposites is known to undergo a dramatic decrease in viscosity,[25] which presumably allows some rearrangement and partial phase separation of the filler within the high volume fraction CNC nanocomposites. An uneven dispersion of CNCs within the nanocomposite will naturally result in variability of mechanical properties across the film. This hypothesis is further supported by the macroscopic phase separation visible in the 20 wt % nanocomposite after it has been subjected to the compression molding procedure. This suggests that there are limitations to the amount of nanofiller that can be homogeneously incorporated into the **1·2** matrix using the processing technique outlined in Figure 2.

After the mechanical properties of the healable supramolecular polymer were shown to be greatly enhanced upon incorporation of CNCs, the next step was to investigate whether broken nanocomposite films can recover their mechanical properties after appropriate thermal treatment. We have shown previously that the matrix (**1·2**) can heal quickly (within seconds) at 80 °C.[25] Thus our initial "healing" procedure for the nanocomposites involved simply taking films which were broken during tensile testing and reprocessing them by compression molding at 200 kPa at 85 °C for 5 min. Stress−strain experiments on the reprocessed films showed that (within experimental error) the films fully recovered (E_R) their original tensile moduli (Table 1 and Figure 4, red squares).

Tensile Healing Study. While the above data show that we can restore the original mechanical properties of the nanocomposites via reprocessing, using such a procedure for *in situ* healing would not be very practical. Thus, to further probe the healing process of the nanocomposites, a second set of experiments was performed which closely followed the healing procedure that we previously reported for the matrix materials **1·2**.[25b] For each nanocomposite formulation, a number of tensile samples were bisected cross-wise with a razor blade and arranged with *ca.* 5 mm of overlap on a PTFE sheet (Figure 5).

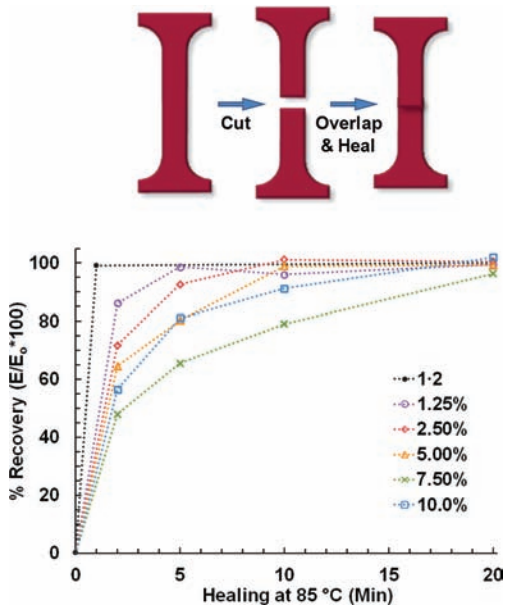

Figure 5. Samples were bisected then overlapped by 5 mm and placed on a PTFE sheet for various times in an oven before being cooled and tested. Percentage recovery of tensile modulus is shown as a function of healing time at 85 °C.

These samples were then heated in an oven at 85 °C for time periods between 2 and 20 min. After cooling, the samples were subjected to tensile testing and compared with undamaged control specimens. It is interesting to note that the large majority of the completely healed films broke outside of the overlap region during the tensile tests. However, it should be pointed out that the thickness of the film in the overlap region will be approximately double that of the rest of the film. Furthermore, the dimensions used to calculate the tensile modulus are that of the films nonoverlapped region and as such the moduli values obtained with this experiment should not be considered as standard tensile moduli. None-the-less as all the films were overlapped to the same extent comparisons of the rate of healing between the different nanocomposites can be made. Figure 5 and Table 2 summarize the results of these experiments and give an estimate of the rate of healing of the nanocomposite series at 85 °C. While all films can be healed to give ≥90% of their original tensile modulus, marked differences

Table 2. Tensile Moduli, E (MPa), As a Function of Healing Time for the Pure Film and the Nanocomposites

Sample	2 min	5 min	10 min	20 min
1·2	8.03 ± 3.20[a]	–	–	8.64 ± 3.64
1·2 + 1.25 wt % CNC	12.8 ± 2.0	14.6 ± 2.3	14.2 ± 2.3	14.7 ± 2.4
1·2 + 2.50 wt % CNC	20.8 ± 4.0	26.8 ± 5.1	29.4 ± 5.6	29.2 ± 5.5
1·2 + 5.00 wt % CNC	41.9 ± 8.8	52.1 ± 10.9	64.1 ± 13.5	64.3 ± 13.5
1·2 + 7.50 wt % CNC	68.4 ± 17.8	93.4 ± 24.3	113 ± 29	137 ± 35
1·2 + 10.0 wt % CNC	150 ± 63	215 ± 90	241 ± 101	270 ± 113

[a]Sample **1·2** recovered its full modulus after less than 1 min at 85 °C.

dx.doi.org/10.1021/ja300050x | J. Am. Chem. Soc. 2012, 134, 5362−5368

in the healing rates are observed. As a general trend, the tensile data show that increasing the proportion of CNCs in the nanocomposite slows the rate of healing, with the 7.50 wt % sample requiring the longest time (*ca.* 20 min) to recover 90% of its original modulus. The only outlier in this data set is the 10.0 wt % CNC sample which displays a faster recovery than the 7.50 wt % film. This observation, however, is consistent with the previous data suggesting the onset of phase segregation at the higher (≥10 wt %) CNC loadings. Thus, in a phase segregated sample the areas containing lower amounts CNC will possess a lower viscosity and heal more quickly, resulting in a faster observed healing rate.

Rheological Healing Study. To achieve a more detailed understanding of the healing of these nanocomposites, we carried out rheological analyses at 65 °C on all of the samples (including the 20.0 wt % CNC nanocomposite). First, the initial moduli of the nanocomposite films were probed at a frequency of 0.1 rad/s and 0.1% of strain. Small frequency and strain values were utilized in order to minimize the deformation and frequency effect on the storage modulus, G′. The results of these experiments are shown in Figure 6, where the initial

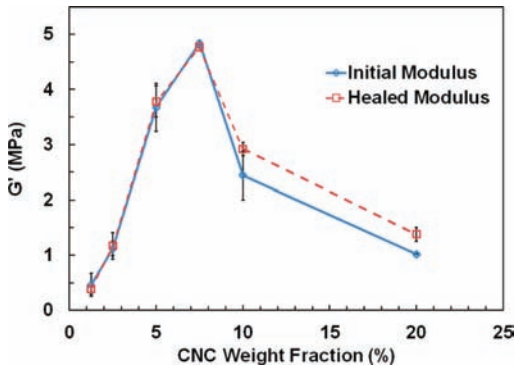

Figure 6. Shear storage modulus versus weight fraction of CNC at 65 °C as determined by rheological analysis.

storage modulus values (blue diamonds) are plotted against CNC weight fraction. As expected from tensile studies, the moduli of the nanocomposites increased with CNC loading up to 7.50 wt %. The nanocomposite with 7.50 wt % CNC showed an order of magnitude higher value of G′ (at 65 °C) when compared to 1.25 wt % CNC nanocomposite films. However, a decrease in the mechanical properties of the films was observed at the higher CNC loading of 10 and 20 wt %, again consistent with phase separation occurring in these films at 65 °C.

After these initial studies the nanocomposite films were deformed via a strain sweep, applying strains from 1% to 100% at 10 rad/s (for the 5.0, 7.5, 10.0, and 20 wt %) or 100 rad/s (for the 1.25 and 2.5 wt %). This deformation process resulted in modulus reduction of 2 to 4 orders of magnitude - consistent with sample breakage. At such large strains, stress−strain responses were in the nonlinear visco-elastic regimes. After the strain sweep, the rehealing ability of the nanocomposites was monitored by a time sweep experiment using a frequency of 0.1 rad/s and a strain of 0.1% in order to minimize the effect of shear on the self-healing process. The time sweep experiment was stopped when the G′ value reached a plateau.

As shown in Figure 6 (red squares) the final, healed, modulus values match very well with the original mechanical properties of all the nanocomposite films at 65 °C. However, the rate of healing of the samples varied considerably as a function of CNC content, which is to be expected given that higher storage modulus values are also indicative of a higher viscosity of the nanocomposites. While 1.25 wt % and 2.50 wt % CNC nanocomposites healed within a minute at 65 °C, the 5.00 wt % CNC sample took about 20 min for complete rehealing to occur. Consistent with the tensile healing data, rehealing of the 7.50 wt % CNC nanocomposite (shown in Figure 7) required

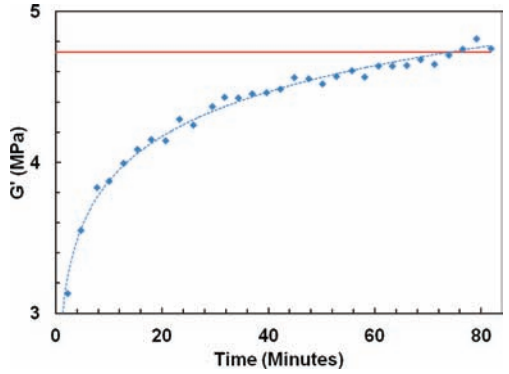

Figure 7. Modulus recovery, as measured by rheometry (ω = 0.1 rad/s, γ = 0.1%) at 65 °C of a broken sample of 7.50 wt % nanocomposite. The initial modulus (red line) was measured at 65 °C at low strain (γ = 0.1%). The sample was then broken using a high frequency strain sweep (ω = 10 rad/s); recovery of the shear storage modulus was monitored at 65 °C over a period of time.

the longest time span (80 min) for full recovery. The measured rheological healing time at 65 °C was about 4 times longer than the time required for healing at 85 °C in tensile studies, highlighting the thermo-responsive nature of this nanocomposite system. The long time required for rehealing of 7.50 wt % CNC nanocomposite may originate from the slow polymer dynamics resulting from a high nanocomposite viscosity. Consistent with macroscopic phase segregation of the nanofiller, as postulated from the tensile healing results, a decrease in both the modulus and rehealing time was observed at CNC loadings greater than 7.50 wt %. The 10.0 wt % and 20.0 wt % CNC samples required about 60 and 1 min respectively for complete rehealing to occur. Overall, the nanocomposite films recovered their initial storage modulus after the healing process and reconstructed the linear stress−strain response (see Supporting Information, Figure S6).

Electron Microscopy. Finally, we also examined the healing process by SEM. In these studies fractured samples were heated from room temperature to 200 °C, at 5 °C min^{-1}, in an environmental scanning electron microscope. In these studies progressive healing with temperature was observed for nanocomposites with the lowest concentration of filler (1.25 wt %; Figure 8; see also Supporting Information Figure S6). At higher CNC concentrations healing rates were too slow due to the dramatic increase in the nanocomposite viscosity for this technique to give useful results. Nonetheless the SEM images of the 1.25 wt % nanocomposite are consistent with the matrix polymer blend dissociating, reducing its viscosity which in turn allows it to heal.

■ CONCLUSION

We have demonstrated reinforcement of a relatively weak but thermally responsive polymer using rigid, biosourced cellulose nanocrystals (CNCs). Nanocomposites were obtained using solvent-based dispersion techniques followed by compression

dx.doi.org/10.1021/ja300050x | *J. Am. Chem. Soc.* 2012, 134, 5362−5368

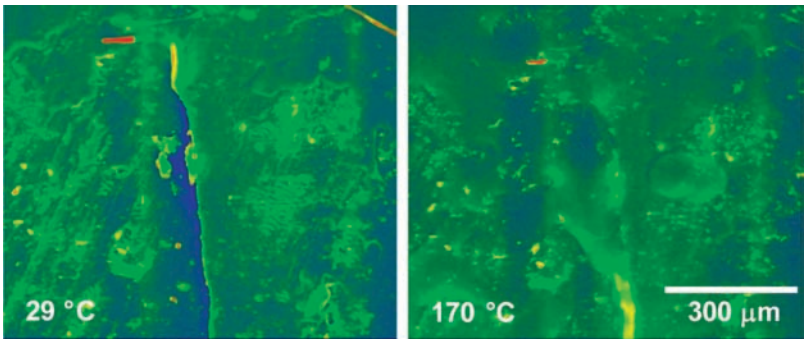

Figure 8. False-color SEM images of the **1·2** + 1.25 wt % CNC composite at 29 and 170 °C. The sample was fractured and then heated to 200 °C, at 5 °C min^{-1}, in an environmental scanning electron microscope (FEI Quanta FEG 600). Original micrographs are reproduced in Supporting Information Figure S6.

molding, and their mechanical and stimuli-response properties were measured as the concentration of reinforcing filler was varied. Increasing the amount of CNC filler dramatically increased the tensile modulus of the films at room temperature (over 30-fold for the 10 wt % CNC nanocomposites). Phase separation does occur above a filler loading of 7.5 wt %, and this has a negative impact on the performance of the composites, resulting in diminished high temperature properties. Nonetheless the healable matrix **1·2** fully maintained its healability with incorporation of CNC nanofiller as shown conclusively by tensile and rheological measurements. It is important to note that the healing rate does depend on the amount of evenly dispersed CNCs (the more CNCs, the slower the healing rate) and the degree of phase separation (the higher the degree of phase separation, the faster the healing rate). These phenomena can be related to the melt viscosity of the nanocomposite with more and evenly dispersed CNCs resulting in higher melt viscosities slowing the ability of the material to fill in cracks and deformations.

■ ASSOCIATED CONTENT

Supporting Information

Isolation procedures and characterization of the CNCs and TGA, the effect of compression molding, rheology and SEM studies of the nanocomposites. This material is available free of charge via the Internet at http://pubs.acs.org.

■ AUTHOR INFORMATION

Corresponding Author

stuart.rowan@case.edu (S.J.R.); mem@udel.edu (M.E.M.)

Notes

The authors declare no competing financial interest.

■ ACKNOWLEDGMENTS

We thank EPSRC and NSF (EP/D07434711, EP/G026203/1, and NSF-DMR-0602869 and NSF-DMR-0804874), the Army Research Office (W911NF-09-1-0145), the University of Reading Research Endowment Trust Fund (a fellowship to S.B.), and the Kent H. Smith Charitable Trust (S.J.R.) for funding of this project. We also thank Dr. Peter J. F. Harris of the Centre for Advanced Microscopy, University of Reading, for help with the SEM studies.

■ REFERENCES

(1) Bergman, S. D.; Wudl, F. *J. Mater. Chem.* **2007**, *18*, 41−62.
(2) Wool, R. P. *Soft Matter* **2008**, *4*, 400−418.
(3) Murphy, E. B.; Wudl, F. *Prog. Polym. Sci.* **2010**, *35*, 223−251.
(4) Burattini, S.; Greenland, B. W.; Chappell, D.; Colquhoun, H. M.; Hayes, W. *Chem. Soc. Rev.* **2010**, *39*, 1973−1985.
(5) Brochu, A. B. W.; Craig, S. L.; Reichert, W. M. *J. Biomed. Mater. Res., Part A* **2011**, *96A*, 492−506.
(6) Ghosh, B.; Urban, M. W. *Science* **2009**, *323*, 1458−1460.
(7) Andersson, H. M.; Keller, M. W.; Moore, J. S.; Sottos, N. R.; White, S. R. Self Healing Materials. In *Self Healing Materials. An Alternative Approach to 20 Centuries of Materials Science*; van der Zwaag, S., Ed.; Springer Series in Material Science; Springer: Dordrecht, The Netherlands, 2005; pp 19−44.
(8) Blaiszik, B. J.; Kramer, S. L. B.; Olugebefola, S. C.; Moore, J. S.; Sottos, N. R.; White, S. R. *Ann. Rev. Mater. Res.* **2010**, *40*, 179−211.
(9) White, S. R.; Sottos, N. R.; Geubelle, P. H.; Moore, J. S.; Kessler, M. R.; Sriram, S. R.; Brown, E. N.; Viswanathan, S. *Nature* **2001**, *409*, 794−797.
(10) See for example: (a) Chen, X.; Dam, M. A.; Ono, K.; Mal, A.; Shen, H.; Nutt, S. R.; Sheran, K.; Wudl, F. *Science* **2002**, *295*, 1698−1702. (b) Scott, T. F.; Schneider, A. D.; Cook, W. D.; Bowman, C. N. *Science* **2005**, *308*, 1615−1617. (c) Amamoto, Y.; Kamada, J.; Otsuka, H.; Takahara, A.; Matyjaszewski, K. *Angew. Chem., Int. Ed.* **2011**, *50*, 1660−1663.
(11) Rowan, S. J.; Cantrill, S. J.; Cousins, G. R. L.; Sanders, J. K. M.; Stoddart, J. F. *Angew. Chem., Int. Ed.* **2002**, *41*, 898−952.
(12) Wojtecki, R. J.; Meador, M. A.; Rowan, S. J. *Nat. Mater.* **2011**, *10*, 14−27.
(13) Wilson, A. J. *Soft Matter* **2007**, *3*, 409−425.
(14) Serpe, M. J.; Craig, S. L. *Langmuir* **2007**, *23*, 1626−1634.
(15) De Greef, T. F. A.; Smulders, M. M. J.; Wolffs, M.; Schenning, A. P. H. J.; Sijbesma, R. P.; Meijer, E. W. *Chem. Rev.* **2009**, *109*, 5687−5754.
(16) Weck, M. *Polym. Int.* **2007**, *56*, 453−460.
(17) Fox, J. D.; Rowan, S. J. *Macromolecules* **2009**, *42*, 6823−6835.
(18) Kim, Y. H.; Wool, R. P. *Macromolecules* **1983**, *16*, 1115−1120.
(19) Cordier, P.; Tournilhac, F.; Soulié-Ziakovic, C.; Leibler, L. *Nature* **2008**, *451*, 977−980.
(20) Montarnal, D.; Tournilhac, F.; Hidalgo, M.; Couturier, J.-L.; Leibler, L. *J. Am. Chem. Soc.* **2009**, *131*, 7966−7967.
(21) Haraguchi, K.; Uyama, K; Tanimoto, H. *Macromol. Rapid Commun.* **2011**, *32*, 1253−1258.
(22) Wang, Q.; Mynar, J. L.; Yoshida, M.; Lee, E.; Lee, M.; Okuro, K.; Kinbara, K.; Aida, T. *Nature* **2010**, *463*, 339−343.
(23) (a) South, A. B.; Lyon, L. A. *Angew. Chem., Int. Ed.* **2010**, *49*, 767−771. (b) Wang, X.; Liu, F.; Zheng, X.; Sun, J. *Angew. Chem., Int. Ed.* **2011**, *50*, 11378−11381.
(24) Burnworth, M.; Tang, L.; Kumpfer, J. R.; Duncan, A. J.; Beyer, F. L.; Fiore, G. L.; Rowan, S. J.; Weder, C. *Nature* **2011**, *472*, 334−337.
(25) (a) Burattini, S.; Colquhoun, H. M.; Greenland, B. W.; Hayes, W. *Faraday Discuss.* **2009**, *143*, 251−264. (b) Burattini, S.; Colquhoun, H. M.; Fox, J. D.; Friedmann, D.; Greenland, B. W.; Harris, P. J. F.;

Hayes, W.; Mackay, M. E.; Rowan, S. J. *Chem. Commun.* **2009**, 6717−6719.
(26) Burattini, S.; Greenland, B. W.; Hayes, W.; Mackay, M. E.; Rowan, S. J.; Colquhoun, H. M. *Chem. Mater.* **2011**, *23*, 6−8.
(27) Burattini, S.; Greenland, B. W.; Merino, D. H.; Weng, W.; Seppala, J.; Colquhoun, H. M.; Hayes, W.; Mackay, M. E.; Hamley, I. W.; Rowan, S. J. *J. Am. Chem. Soc.* **2010**, *132*, 12051−12058.
(28) Greenland, B. W.; Burattini, S.; Hayes, W.; Colquhoun, H. M. *Tetrahedron* **2008**, *64*, 8346−8354.
(29) Orts, W. J.; Shey, J.; Imam, S. H.; Glenn, G. M.; Guttman, M. E.; Revol, J. F. *J. Polym. Environ.* **2005**, *13*, 301−306.
(30) Favier, V.; Chanzy, H.; Cavaille, J. *Macromolecules* **1995**, *28*, 6365−6367.
(31) Jordan, J.; Jacob, K. I.; Tannenbaum, R.; Sharaf, M. A.; Jasiuk, I. *Mater. Sci. Eng., A* **2005**, *393*, 1−11.
(32) Eichhorn, S. J. *Soft Matter* **2011**, *7*, 303−315.
(33) Eichhorn, S. J.; Dufresne, A.; Aranguren, M.; Marcovich, N. E.; Capadona, J. R.; Rowan, S. J.; Weder, C.; Thielemans, W.; Roman, M.; Renneckar, S.; Gindl, W.; Veigel, S.; Keckes, J.; Yano, H.; Abe, K.; Nogi, M.; Nakagaito, A. N.; Mangalam, A.; Simonsen, J.; Benight, A. S.; Bismarck, A.; Berglund, L. A.; Peijs, T. *J. Mater. Sci.* **2010**, *45*, 1−33.
(34) Habibi, Y.; Lucia, L. A.; Rojas, O. J. *Chem. Rev* **2010**, *110*, 3479−3500.
(35) Capadona, J. R.; Shanmuganathan, K.; Tyler, D. J.; Rowan, S. J.; Weder, C. *Science* **2008**, *319*, 1370−1374.
(36) Ben Azouz, K.; Ramires, E. C.; Van den Fonteyne, W.; El Kissi, N.; Dufresne, A. *Macro Lett.* **2012**, *1*, 236−240.
(37) Šturcová, A.; Davies, G. R.; Eichhorn, S. J. *Biomacromolecules* **2005**, *6*, 1055−1061.
(38) Ott, E.; Spurlin, H. M.; Grafflin, M. W. *Cellulose and Cellulose Derivatives*; Interscience Publishers: New York, 1954; Vol. *5*.
(39) van den Berg, O.; Capadona, J. R.; Weder, C. *Biomacromolecules* **2007**, *8*, 1353−1357.
(40) de Souza Lima, M. M.; Wong, J.; Paillet, M.; Borsali, R.; Pecora, R. *Langmuir* **2003**, *19*, 24−29.
(41) Favier, V.; Chanzy, H.; Cavaillé, J. Y. *Macromolecules* **1995**, *28*, 6365−6367.
(42) Shanmuganathan, K.; Capadona, J. R.; Rowan, S. J.; Weder, C. *Prog. Polym. Sci.* **2010**, *35*, 212−222.
(43) van den Berg, O.; Capadona, J. R.; Weder, C. *Biomacromolecules* **2007**, *8*, 1353−1357.
(44) Ouali, N.; Cavaille, J. Y.; Perez, J. *Plast., Rubber Compos. Process Appl.* **1991**, *16*, 55−60.
(45) Takayanaki, M.; Uemura, S.; Minami, S. *J. Polym. Sci., Part C* **1964**, *5*, 113−122.
(46) Capadona, J. R.; Van Den Berg, O.; Capadona, L. A.; Schroeter, M.; Rowan, S. J.; Tyler, D. J.; Weder, C. *Nat. Nanotechnol.* **2007**, *2*, 765−769.